Generation of Multiple Mid Infrared Wavelengths Using PPLN and $AgGaSe_2$

Ti Chuang, Nigel Martin and Ralph Burnham

Fibertek, Inc. 510 Herndon Parkway, Herndon, VA 20170

ABSTRACT

We report the demonstration of simultaneously generating two mid infrared wavelengths using both PPLN and $AgGaSe_2$ nonlinear materials pumped by a KTP OPO at 1.54 μm. In either case, the signal and idler waves were near 2.5 μm and 4.0 μm. The architecture we chose is capable of producing three important IRCM wavelength bands near 2.5, 3.5 and 4.0 μm in the mid infrared region, and of providing rapid wavelength tuning when all PPLN OPOs are used. The experiment reported here with PPLN shows better performance over that with $AgGaSe_2$ and is, to the best of our knowledge, the first such multiband OPO operation with PPLN. In initial experiments with PPLN, we obtained output powers of 542 mW and 453 mW near 2.5 μm and 4.0 μm, with conversion efficiencies of 30% and 25% respectively. The combined MIR output was 995 mW with a combined conversion efficiency of 55%.

1 INTRODUCTION

In the area of active infrared countermeasures, a mid infrared (MIR) laser source that is wavelength agile and capable of producing multiple wavelengths from 2.5 μm to 4 μm is a necessary device to achieve the most effective protection of aircraft with the highest versatility. One excellent architecture to produce such a laser source is to employ multiple stages of optical parametric oscillators (OPO) pumped by an efficient solid state laser source. We have demonstrated this architecture by using two different approaches. Both approaches start with a diode-pumped Nd based fundamental pump source oscillating near 1 μm. The laser pumps either a KTP or a KTA OPO, with noncritically phase matching (NCPM), to generate a wavelength at 1.54 μm. This 1.54 μm source becomes the pump for the second OPO that generates two MIR bands near 2.5 and 4.0 μm. The difference in these two approaches lies in the material selection

REPORT DOCUMENTATION PAGE

Form Approved OMB No. 0704-0188

1. REPORT DATE (DD-MM-YYYY)	2. REPORT TYPE	3. DATES COVERED (FROM - TO)
01-01-1998	Conference Proceedings	xx-xx-1998 to xx-xx-1998

4. TITLE AND SUBTITLE
Generation of Multiple Mid Infrared Wavelengths Using PPLN and AgGaSe2
Unclassified

5a. CONTRACT NUMBER
5b. GRANT NUMBER
5c. PROGRAM ELEMENT NUMBER

6. AUTHOR(S)
Chuang, Ti ;
Martin, Nigel ;
Burnham, Ralph ;

5d. PROJECT NUMBER
5e. TASK NUMBER
5f. WORK UNIT NUMBER

7. PERFORMING ORGANIZATION NAME AND ADDRESS
Fibertek, Inc.
510 Herndon Parkway
Herndon, VA20170

8. PERFORMING ORGANIZATION REPORT NUMBER

9. SPONSORING/MONITORING AGENCY NAME AND ADDRESS
Director, CECOM RDEC
Night Vision and Electronic Sensors Directorate, Security Team
10221 Burbeck Rd.
Ft. Belvoir, VA22060-5806

10. SPONSOR/MONITOR'S ACRONYM(S)
11. SPONSOR/MONITOR'S REPORT NUMBER(S)

12. DISTRIBUTION/AVAILABILITY STATEMENT
APUBLIC RELEASE
,

13. SUPPLEMENTARY NOTES
See Also ADM201041, 1998 IRIS Proceedings on CD-ROM.

14. ABSTRACT
We report the demonstration of simultaneously generating two mid infrared wavelengths using both PPLN and AgGaSe2 nonlinear materials pumped by a KTP OPO at 1.54 mm. In either case, the signal and idler waves were near 2.5 mm and 4.0 mm. The architecture we chose is capable of producing three important IRCM wavelength bands near 2.5, 3.5 and 4.0 mm in the mid infrared region, and of providing rapid wavelength tuning when all PPLN OPOs are used. The experiment reported here with PPLN shows better performance over that with AgGaSe2 and is, to the best of our knowledge, the first such multiband OPO operation with PPLN. In initial experiments with PPLN, we obtained output powers of 542 mW and 453 mW near 2.5 mm and 4.0 mm, with conversion efficiencies of 30% and 25% respectively. The combined MIR output was 995 mW with a combined conversion efficiency of 55%.

15. SUBJECT TERMS

16. SECURITY CLASSIFICATION OF:			17. LIMITATION OF ABSTRACT	18. NUMBER OF PAGES	19. NAME OF RESPONSIBLE PERSON
a. REPORT	b. ABSTRACT	c. THIS PAGE	Public Release	15	Fenster, Lynn lfenster@dtic.mil
Unclassified	Unclassified	Unclassified			19b. TELEPHONE NUMBER International Area Code Area Code Telephone Number 703767-9007 DSN 427-9007

for the second (MIR) OPO. The first material selection is Periodically Poled Lithium Niobate (PPLN), which utilizes quasi-phase matching (QPM). The second is Silver Gallium Selenide ($AgGaSe_2$ - AGSe), which utilizes birefringent phase matching.

2 PPLN OPTICAL PARAMETRIC OSCILLATOR

Periodically polled lithium niobate is a promising material for nonlinear optics applications, such as second harmonic generation (SHG) [1] and optical parametric oscillation. [2] PPLN devices rely on quasi-phase matching to realize nonlinear frequency conversion. Even though the concept of QPM was proposed by Armstrong and Bloembergen et al. in 1962 and 1970 respectively, [3] it was not until the beginning of the 90s that the technology would allow the concept to become practical. A common OPO application of this kind is to employ the mature Nd doped laser sources near 1.0 μm as the fundamental pump source to generate an idler wave between 3 and 4 μm region of mid infrared. [4] This approach has been shown to be very efficient, but normally produces only one wavelength at a time in the MIR region between 2.5 and 4 μm along with another one near 1.5 μm in the near infrared (NIR) region.

In our experiments, we combined two technologies together. The first is the utilization of a birefringently phase matched OPO using nonlinear crystals like Potassium Titanyl Phosphate (KTP) and Potassium Titanyl Arsenate (KTA). The second is the quasi phase matched OPO process provided by PPLN material. Two OPO processes operate in tandem, in which the birefringently phase matched OPO serves as the first stage, providing the pump source for the second OPO in PPLN. We used an NCPM OPO with a KTP crystal, pumped by a Nd:YLF laser oscillating at 1.047 μm, to generate a signal wave at 1.54 μm in NIR region. The 1.54 μm NIR laser serves as the pump source for the PPLN OPO, which produced signal and idler waves near 2.5 μm and 4.0 μm in the MIR region. Both signal and idler waves are tunable by choosing a proper grating period and the operating temperature of the PPLN.

The layout of the multiband PPLN MIR source is shown in Fig. 1. It consisted of a 1.54 μm KTP OPO and a PPLN OPO. The former contained a fundamental 1.047 μm pump laser and a monolithic KTP OPO. A focusing lens was positioned between KTP OPO and PPLN OPO for pump mode matching. The fundamental Nd:YLF laser was continuously pumped by two cw diode bars, and was repetitively Q-switched by an A-O Q-switch at a typical rate of 15 KHz. The NIR OPO laser was an intracavity, monolithic KTP OPO. The noncritical phase matching of KTP was chosen because of high efficiency and no walk off associated with NCPM. In our experiments, the average output power of the NIR OPO at 1.54 μm was between 1.5 and 2.0 W. The pulsewidth of the NIR OPO was around 5 ns. The wavelengths measured for the NIR OPO was near 1.5398 ± 0.00035 μm (signal wave). Since the pump beam quality at 1.54 μm has great influence to the performance of the subsequent OPO, we made extreme effort to ensure good

beam quality of the 1.54 μm pump beam. Fig. 2 illustrates the beam profile of the 1.54 μm pump beam. As can be seen in Fig. 2, the beam image and contour were fairly circular, with nearly Guassion profiles in the two perpendicular orientations. A typical M^2 value of the beam was less than 1.5 .

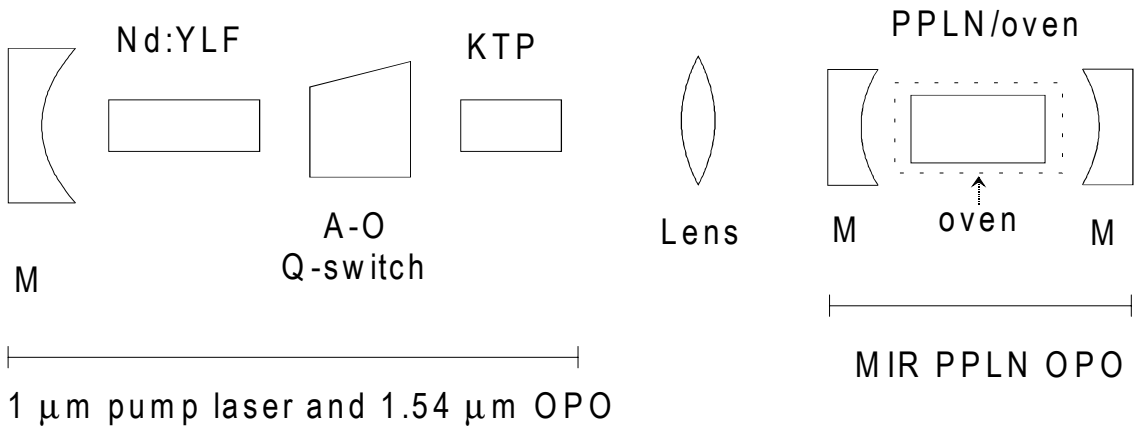

Fig. 1 Layout of the multiband PPLN MIR laser source. M: mirrors.

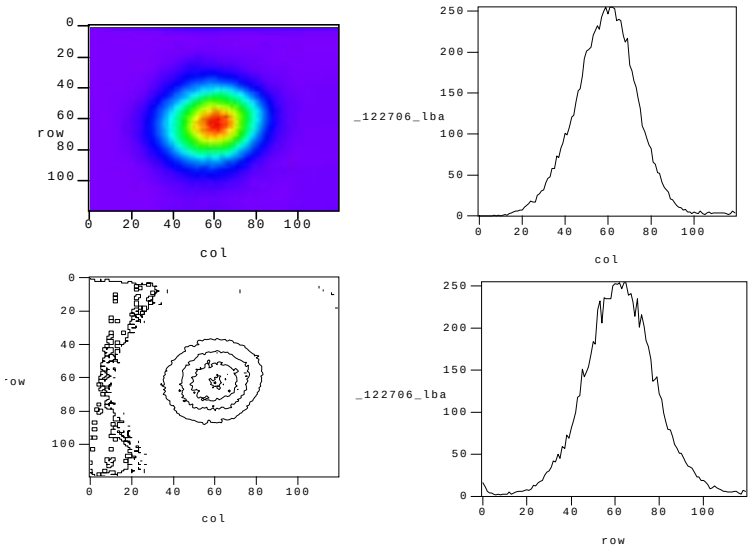

Fig. 2 The beam image, image contour and beam profiles of the 1.54 μm pump beam.

The focusing lens shown in Fig. 1 had a focal length of 50 mm. The lens focused the pump beam to approximately a 100 μm diameter spot at the center of the PPLN crystal. The MIR laser resonator was symmetrical, and was composed of two curved mirrors with equal radii of curvature of 10 cm. The PPLN sample with its temperature oven was placed roughly at the middle of the resonator. The separation between the input and output mirrors was 25 mm. The

input mirror had a transmission > 90% at 1.54 μm, and a reflection >95% between 2.5 and 4.0 μm. The output coupler (OC) had a high reflectivity at the pump wavelength of 1.54 μm, a 10% transmission at 2.5 μm and a 98% transmission at 4.0 μm. The second face of the OC was not AR coated. The PPLN OPO resonator was singly resonant at the signal wave near 2.5 μm. The pump beam made a complete round trip inside the resonator.

The PPLN sample was fabricated by Crystal Technology, Inc (CTI) in Palo Alto, CA, with five grating periods: 31.9 μm, 32.1μm, 32.3μm, 32.5 μm and 32.7 μm. The PPLN sample had dimensions of 19 mm x 11 mm x 0.5 mm (length x width x thickness) . The end faces of the sample (11 mm x 0.5 mm) were AR coated near three wavelengths of interest: 1.54 μm, 2.5 μm and 4.0 μm. We placed the PPLN sample in an oven primarily for temperature tuning, while it also provided some degree of prevention from photo refractive damage, although in the NIR wavelength region this damage is not as great as that in the visible region. In the early stage of experiments we observed the second, third and fourth harmonic generation of the pump wavelength (1.54 μm) with the PPLN sample at 770 nm, 513 nm and 385 nm respectively. A schematic of the PPLN sample is depicted in Fig. 3. The beams of the pump, signal and idler propagated along the direction of the 19 mm dimension, with their polarizations all parallel to the optical axis (eee polarization). This arrangement utilized the high nonlinear coefficient d_{33} of $LiNbO_3$ (27 pm/V) , and provided the first order QPM effective nonlinear coefficient of $d_Q = (2/\pi\ d_{33}) = 17$ pm/V.[5] We calculated the temperature tuning curves of the sample for the idler wavelength.[6] The results are given in Fig. 4, which indicates that we can reach the idler wave near 4.0 μm at two grating periods with two temperature points.

Fig. 3 Dimensions and grating periodicities of the PPLN sample

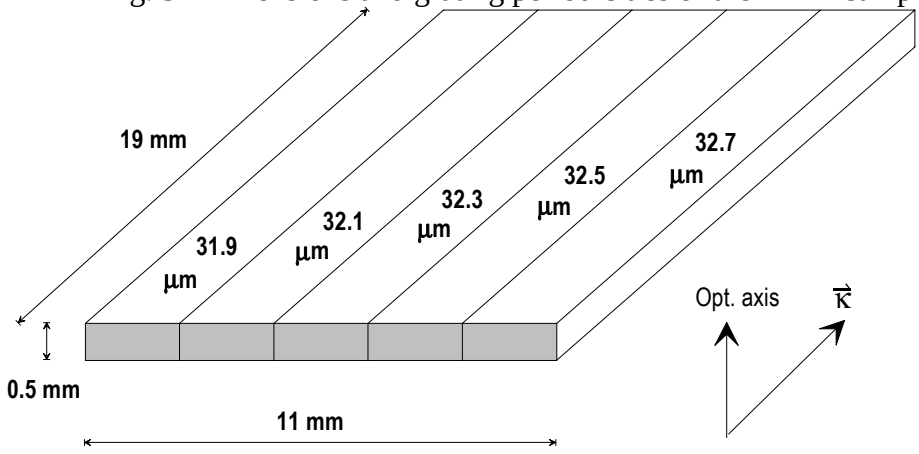

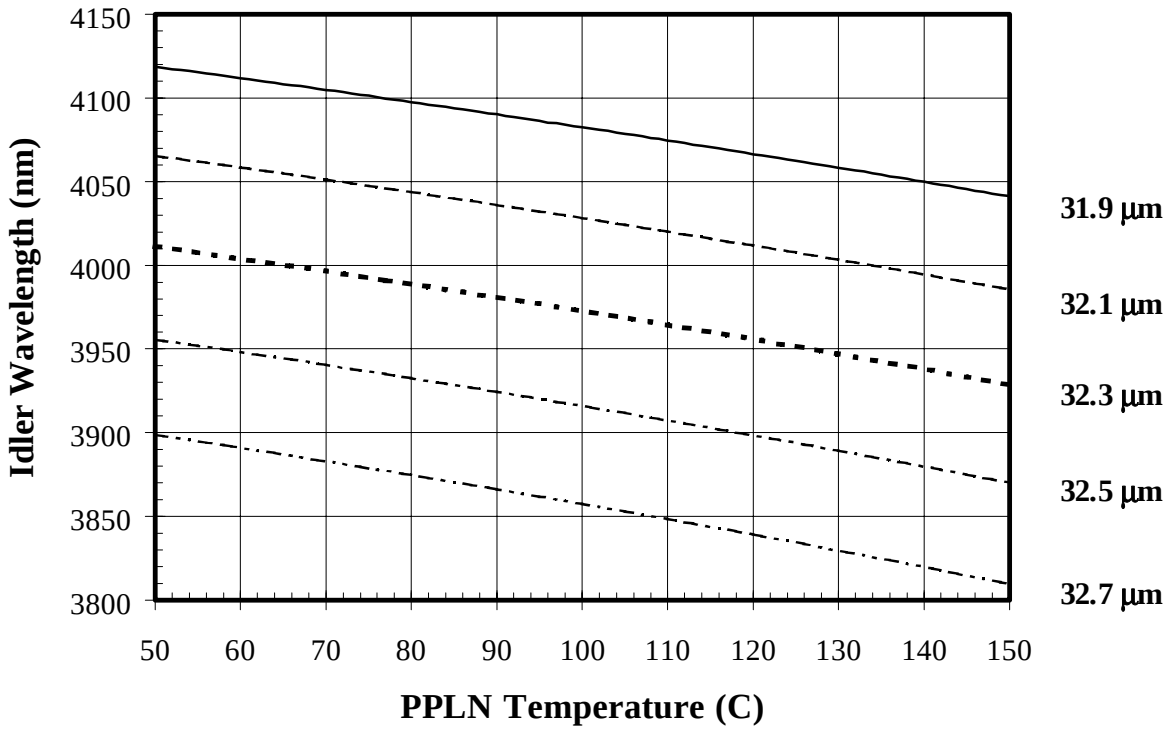

Fig. 4 Calculated temperature tuning curves for idler waves of the PPLN sample. It shows two operating points to reach the idler wavelength near 4.0 μm.

Our first experiment was to measure the wavelength tuning with different grating periods and temperature. The results are presented in Figs. 5 and 6, in which experimental data are compared with theoretically calculated tuning curves given in Fig. 4. In Fig. 5 we show the data taken at the grating period of 32.3 μm with a temperature scan from 29 ^{o}C to 138 ^{0} C. The agreement between the measured data and calculated data is extremely good except at the higher temperature and at the longer idler wavelength. This discrepancy is basically due to the fitting of Sellmeier coefficients, which tend to be less accurate at the higher temperature and longer wavelengths. In Fig. 6 we show the similar wavelength tuning results with all five grating periods at 69 ^{o}C and 139 ^{o}C. As in Fig. 5, the agreement between the experimental data and calculated tuning curves is better at the lower temperature and shorter wavelength.

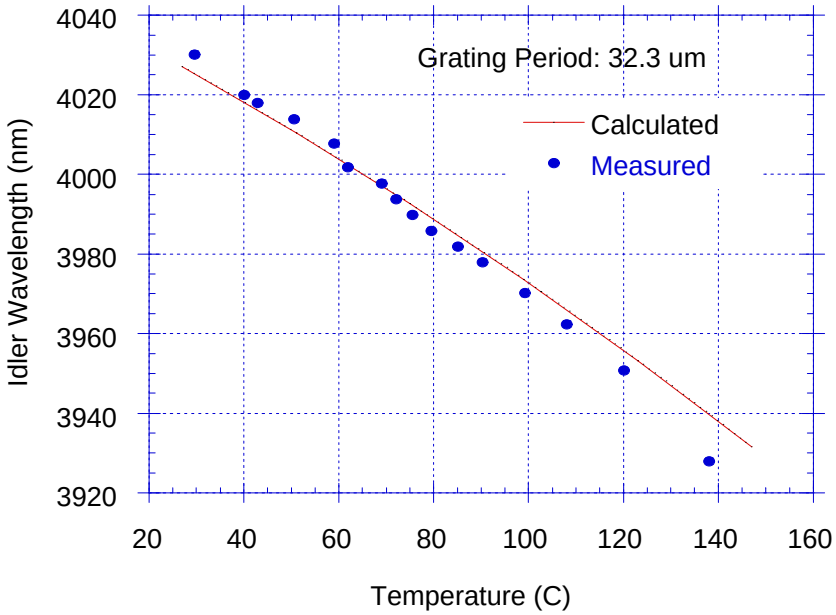

Fig. 5 The calculated temperature tuning curve and experimental data for the grating period of 32.3 μm

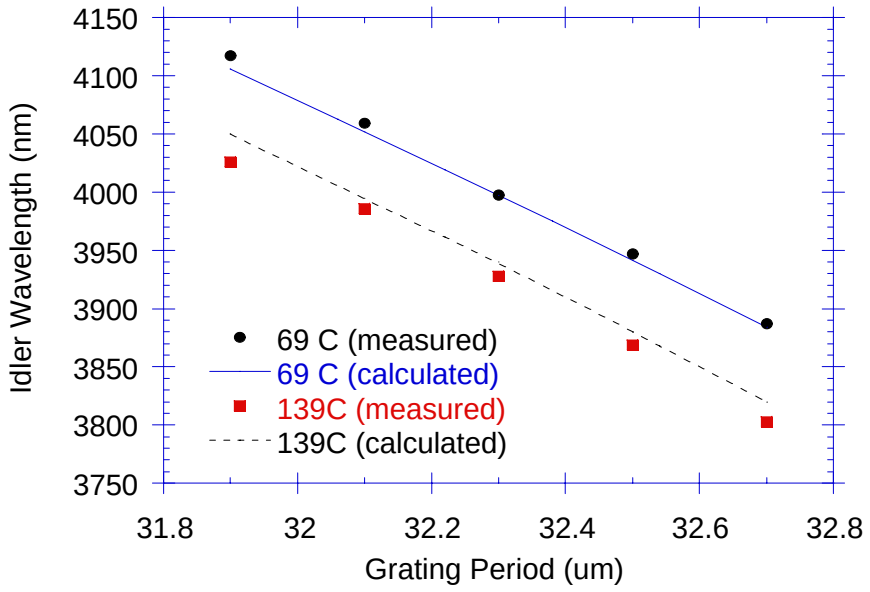

Fig. 6 Calculated temperature tuning curves and experimental data for five grating period at two temperature points.

The wavelength measurements presented in Figs. 5 and 6 were performed with a Thermo

Jarrell Ash 0.4 meter monochromator. It was calibrated using three wavelengths available from the Nd:YLF pump laser and the KTP OPO: 523.5 nm, 1047 nm and 1540 nm, and their second order diffractions. The calibration accuracy was ± 0.8 nm or better. We measured the signal wavelengths (near 2.5 μm) with the monochromator. The idler wavelengths, which were presented in Figs. 5 and 6, were derived from the measurements using the relationship: $1/\lambda_p = 1/\lambda_s + 1/\lambda_i$, where λ_p , λ_s and λ_i are pump, signal and idler wavelengths. In both Figs. 5 and 6 the size of experimental data points is indicative of the experimental accuracy. We used a InSb detector, cooled to 77 K temperature, to detect the weak signal after the monochromator.

The power performance of the multiband PPLN MIR source is presented in Fig. 7. Two sets of data are shown there. One is the input - output curve for the signal at 2504.9 nm, and the other, for the idler at 3997.8 nm. With a pump power of 1.8 W, we obtained the signal power of 542 mW and the idler power of 453 mW (corrected for the loss on the uncoated face of the OC). The slope efficiencies, as shown in Fig. 7, are 42.9% for the signal and 35.6% for the idler respectively. The threshold pump power was approximately 0.57 W, obtained by extrapolating the curves in Fig. 7. The combined power output of both signal and idler was 995 mW, corresponding to a 78.3% slope efficiency.

Fig. 7 Power performance of the multiband PPLN MIR OPO for both signal and idler waves.

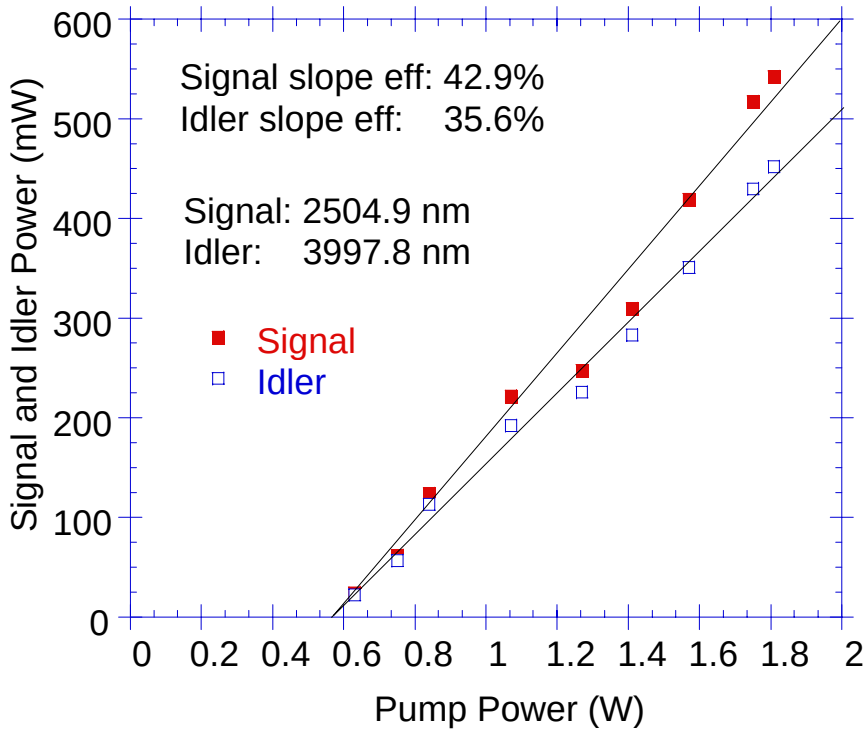

The conversion efficiency of the PPLN MIR OPO, which is defined as the ratio of the output power of either signal or idler to the input pump power, is plotted in Fig. 8. In this figure the solid and open squares are experimental data for signal and idler waves. The maximum conversion efficiencies as shown from the data are 30% and 25% for signal and idler waves. Since the combined output power of two MIR bands is 995 mW, the combined conversion efficiency is 55%. The solid and dashed lines in Fig. 7 are the fitted curves for the signal and idler conversion efficiencies: P_s,P_i /P_p, where P_s and P_i are either the signal or idler output power and P_p is the pump power. The P_s and P_i here are derived from the least square fits of the signal and idler output powers obtained from Fig. 7. Both curves in Fig. 8 show a trend of monotonic increase. There is no indication of back conversion at the highest pump power. We believe scaling to higher power with this PPLN OPO is possible, which will be carried out in the future experiments. It is interesting to note that the pump intensity is near 200 MW/cm^2 at 1.8 W input. This intensity is comparable to the nominal damage threshold for the $LiNbO_3$ crystal measured at 1.06 mm wavelength. However, damage was not observed at this pump intensity in our experiments.

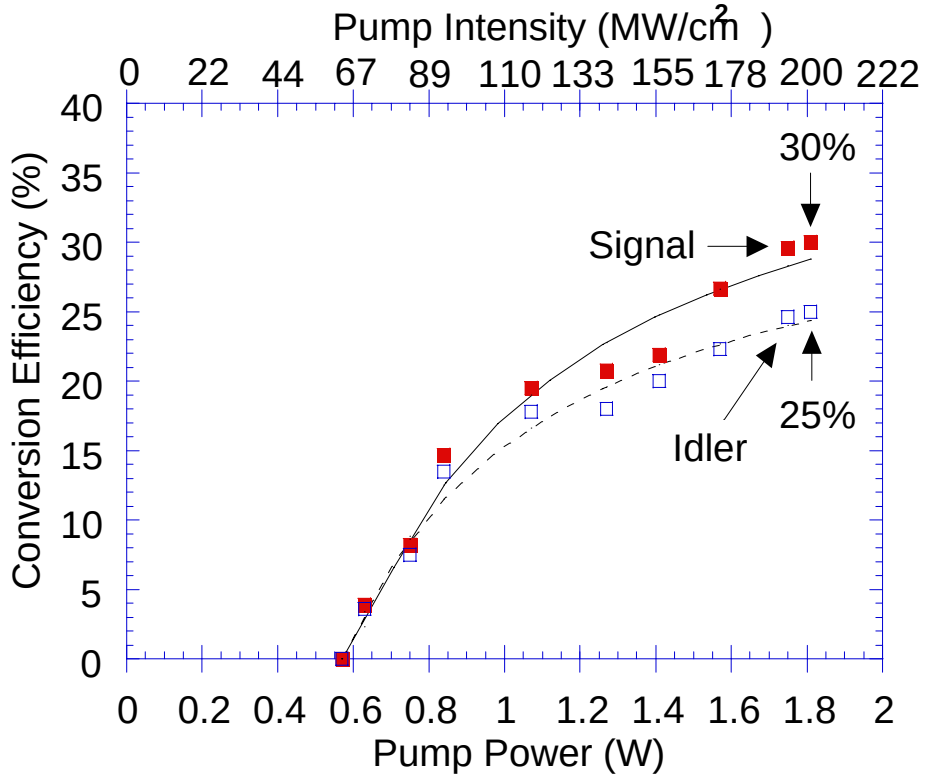

Fig. 8 Conversion efficiencies of the multiband PPLN MIR OPO for both signal and idler waves as the function of pump power and pump intensity.

We also carried out a measurement to determine the beam property (M^2 value) of the signal wave at 2.5 mm. A positive lens was placed in the signal beam, and focused the beam to

a new beam waist. We applied the knife edge method to measure the beam diameters at several positions before and after the new beam waist. The M^2 value of the signal wave was deduced from the measurement to be 2.3 x diffraction-limited ($M^2 = 2.3$) of a Gaussian beam.

In order to better understand the performance of the PPLN MIR OPO, particularly to determine if a higher conversion efficiency could be obtained to produce more output power, we make the following heuristic argument. Assume that at above the threshold of an OPO every pump photon is completed converted to a signal and a idler photon. When this takes place, the conversion efficiency, defined as quantum efficiency, is said to be 1. This quantum efficiency is the theoretical limit of the OPO. Applying this argument to our case, we examine the analysis to the idler wavelength. We then have this equation: $P_p \lambda_p = P_i \lambda_i$, where P is the power, λ is the wavelength and subscripts of p and i represent the pump and the idler. Using λ_p =1540 nm and λ_i = 4000 nm, the ratio of P_i to P_p is 0.385 when the quantum efficiency is 1. From our experimental results, this ratio is found to be 0.252. This experimental value is 65% of the theoretical limit. Therefore, it appears to us that we will still be able to improve the conversion efficiency and increase the output power of both signal and idler waves. One particular area that we believe can be improved is the HR coating for both signal and idler at the input mirror of the OPO resonator. Also, using a confocal resonator configuration for the PPLN OPO will result in a better performance.

3 $AgGaSe_2$ OPTICAL PARAMETRIC OSCILLATOR

Silver Gallium Selenide ($AgGaSe_2$, AGSE) is an excellent material for an MIR OPO when pumped at 1.54 µm.[7] This pump wavelength avoids the strong bulk absorption that AgGaSe2 material has at 2 µm. Therefore, better performance can be achieved with the pump wavelength at 1.54 µm, as compared to that at 2 µm. In addition, the Type I phase matching angle is near 90^o, which provides the benefit of noncritical phase matching.

We also performed experiments using a AGSE crystal as the MIR nonlinear material. Fig. 9 shows the block diagram of the AGSE MIR laser source, including the fundamental and 1.54 µm pump lasers. The fundamental pump laser and KTP OPO are identical to those used in PPLN multiband MIR laser experiments. After passing through a focusing lens of 10 cm focal length, which provided basically a 1:1 imaging, the NIR pump beam impinged on the AGSE OPO crystal, with a beam spot of 660 µm in diameter inside the nonlinear crystal. The MIR laser resonator was composed of a flat input mirror, a AGSE crystal and a flat output coupler. The optimal separation between the input and output mirrors was about 60 mm. The input mirror had a transmission > 90% at 1.54 µm, and a reflection >95% between 2.5 and 4 µm. The output coupler had a high reflectivity at the pump wavelength of 1.54 µm, a 10% transmission at 2.5 µm and a 98% transmission at 4.0 µm. The second face of the output coupler had a broad band AR

coating between 2.5 and 4.0 µm. This OPO resonator was singly resonant at the signal wave of 2.5 µm. The pump beam made a complete round trip inside the resonator.

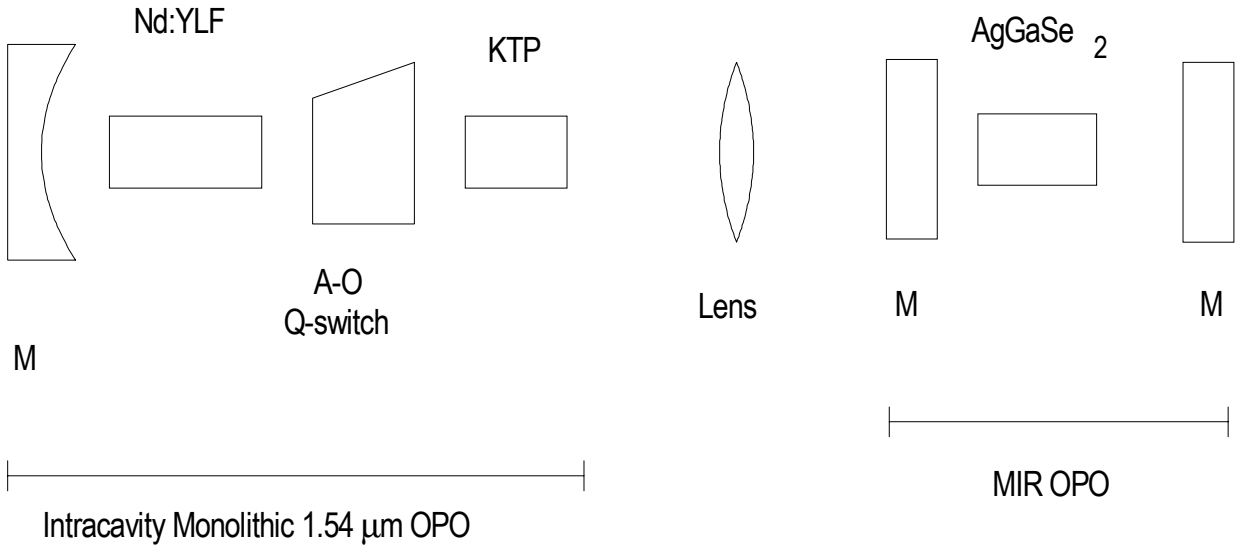

Fig. 9 The layout of the MIR laser source with an $AgGaSe_2$ crystal as second OPO. M: mirrors

The dimensions of the AgGaSe2 crystal were 4 x 4 x 30 mm, with Type I phase matching angles at $\theta = 81.3^o$ and $\phi = 45^o$. The coatings on the entrance and exit faces of the materials were AR at 1.54 µm and broad band AR from 2.4 to 4.1 µm. The nominal reflectivities are less than 0.5% at 1.54 µm, 8% at 2.5 µm and 1% at 4 µm. The polarizations of the pump, signal and idler waves were "eoo", which led to an effective nonlinear coefficient of $d_{eff} = d_{36} \sin\theta \sin 2\phi = 32.6$ pm/V, where $d_{33} = 33$ pm/V [8] Fig. 10 provides the dimensions and cut angle θ for the AGSE crystal.

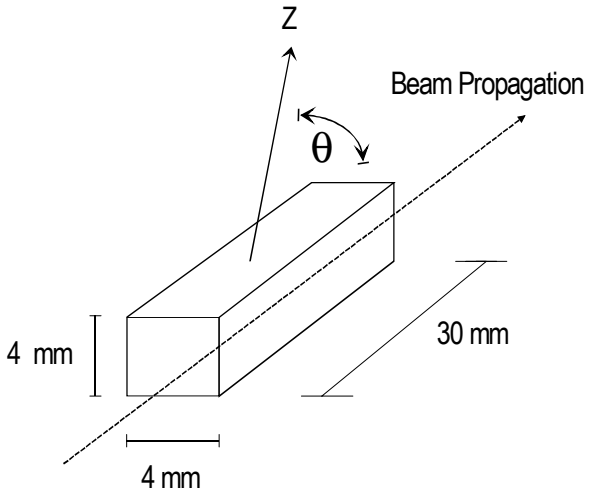

Fig. 10 Dimensions and cut angle θ for the AGSE crystal

A typical power performance curve of the AGSE MIR OPO is presented in Fig. 11. At the pump power of 1.5 W at 1.54 µm, the output power at 2.5 µm was 330 mW, while that at 4.0 µm was 280 mW. The AGSE OPO had an extremely low pump power threshold, less than 50 mW. The slope efficiencies are 21% and 18%, respectively, at 2.5 µm and 4.0 µm. The wavelength of the AGSE OPO was measured to be between 3.97 and 4.03 µm for the idler wave, with signal waves near 2.5 µm.

Fig. 11 Power performance of AGSE MIR OPO for both signal and idler waves

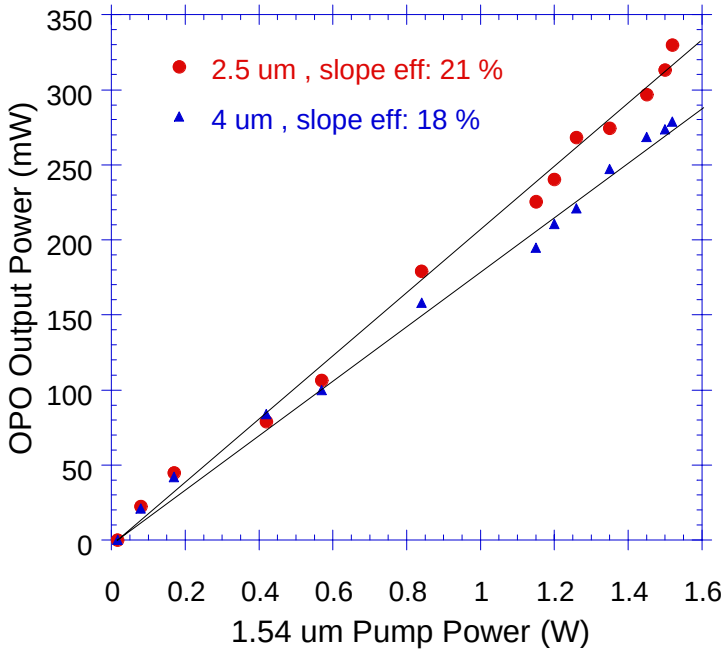

The conversion efficiency of the AGSE MIR OPO is given in Fig. 12. Similar to Fig. 8, solid and open circles shown in Fig. 12 are experimental data for signal and idler waves respectively. The conversion efficiencies at pump power of 1.5 W are 21% and 18% for signal and idler waves. The solid and dashed lines in Fig. 11 are fitted conversion efficiency curves for signal and idler waves, and are obtained using the same method that led to two fitted curves given in Fig. 8. Unlike the two fitted curves in Fig. 7, two fitted curves in Fig. 11 reach saturation quickly at 0.2 W of pump power, which is about 5 times above the threshold, and remain constant afterwards. The conversion efficiencies approach the corresponding slope efficiencies of signal and idler waves . The beam quality at 4.0 mm was measured to be 3 x diffraction-limited ($M^2 = 3$).

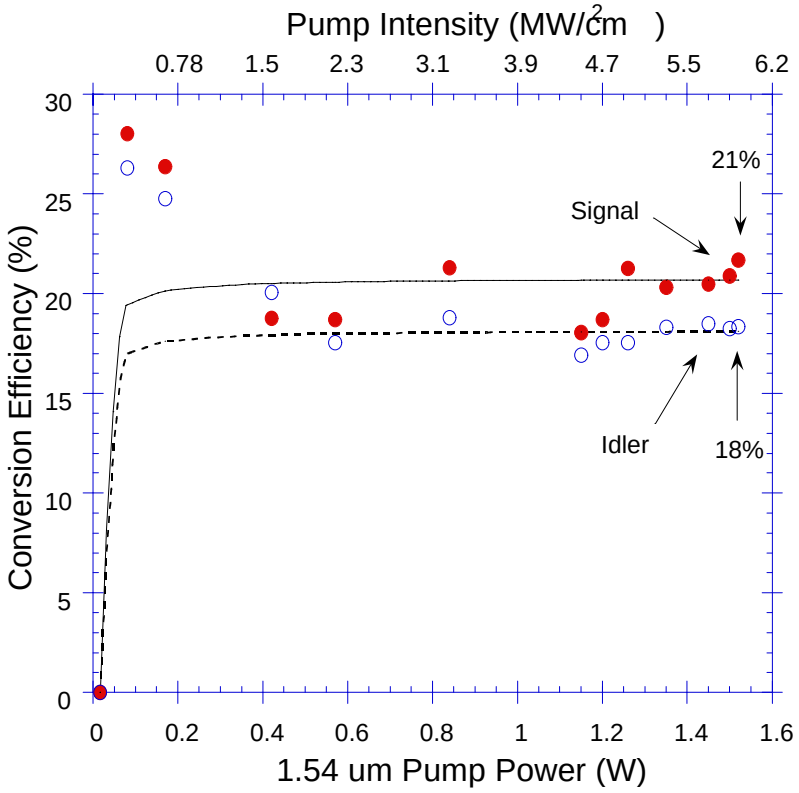

Fig. 12 Conversion efficiencies of the AGSE MIR OPO for both signal and idler waves as the function of pump power and pump intensity

We applied the same argument as outlined at the end of Section 2 to the AGSE MIR OPO. We found the ratio of P_i to P_p in the AGSE OPO experiment to be 0.18, which is 47% of the theoretical ratio of 0.385. This seems to indicate that it would be still possible to achieve

higher conversion efficiency with AGSE. However, the behaviors of two curves shown in Fig. 12 point to the opposite that higher conversion efficiency is not obtainable. We attributed this to the material quality of AGSE and the thermal lensing observed inside AGSE when pump power was increased.

4 LASER PACKAGING AND HARDWARE

Both PPLN MIR laser and the AGSE MIR laser are packaged to a size of 25 cm x 10 cm x 5 cm with a weight of 1.6 Kg. The package is air-cooled, and has passed flight qualification test. The package was designed to fit the existing IRCM hardware without any other re-engineering of the hardware. Fig. 13 shows a photo of the laser package, which has been integrated with its control electronics and cooling fan, as shown in Fig. 14.

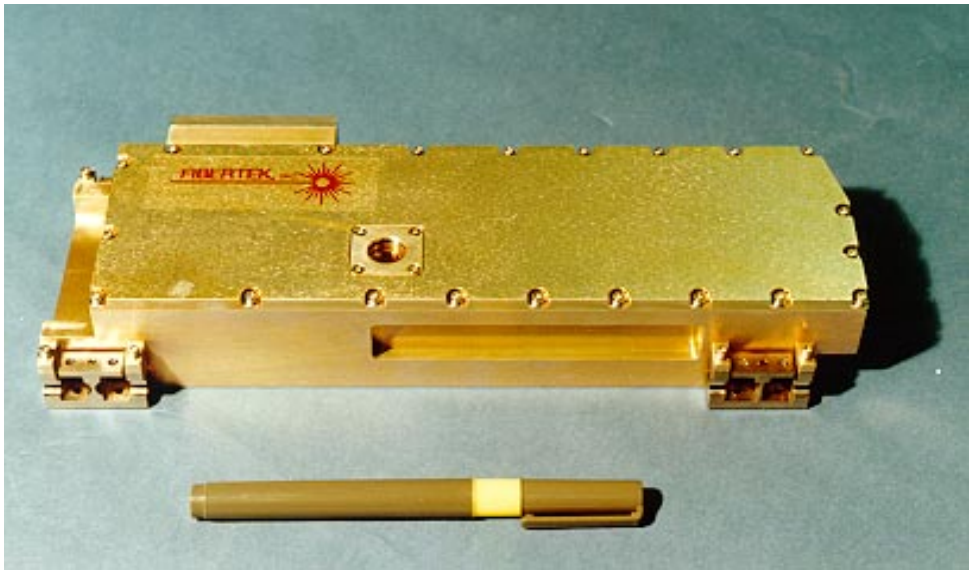

Fig. 13 Photo of the MIR laser packaging

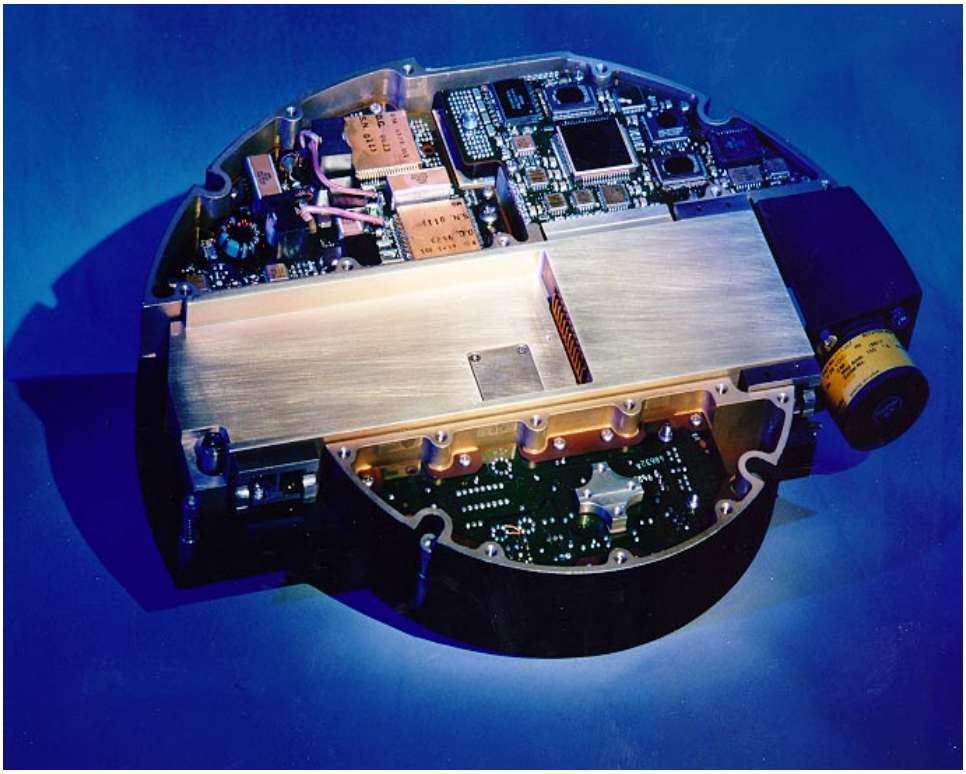

Fig. 14 Photo of the integrated MIR laser with its control electronics. The integrated configuration provided a fan for cooling the MIR laser. Curtesy of Northrop Grumman Corporation.

5 CONCLUSIONS

We have demonstrated the simultaneous generation of MIR output between 2.5 μm and 4 μm using both PPLN and $AgGaSe_2$ nonlinear materials pumped at 1.54 μm. The results indicate that PPLN is a better martial for this application compared to AGSE, even though ASGE possesses a higher effective nonlinear coefficient. PPLN shows the potential of achieving higher OPO power output and conversion efficiency.

The architecture illustrated here can be extended to produce three MIR wavelengths between 2.5 and 4.0 μm by using a PPLN OPO pumped by a 1.54 mm KTA OPO, which generates an idler wave near 3.5 μm. Furthermore, this architecture can use PPLN as the first stage OPO to achieve rapid and wide wavelength tuning of its output wavelength. Then, in addition to its own wavelength tunability enabled by the grating period selection and temperature tuning, the second PPLN OPO is allowed extra wavelength tunability through the wavelength

tuning of its pump. Future experiments are planned to scale up the output power to 2 W at each band of 2.5 μm, 3.4 μm and 4.0 μm in a compact and lightweight configuration.

References

1 D.H. Jundt, G.A. Magel, M.M. Fejer and R.L. Byer, Appl. Phys. Lett. 59, (21), 2657 (1991); M.M. Fejer, G.A. Magel, D.H. Jundt, and R.L. Byer, IEEE J. Qunt. Elect. 28, No.11, 2631 (1992).

2 L.E. Myers, G.D. Miller, R.C. Eckardt, M.M. Fejer and R.L. Byer, Opt. Lett. 20, No. 1, 52 (1995); L.E. Myers, R.C. Eckardt, M.M. Fejer, and R.L. Byer, W.R. Bosenberg, J. W. Pierce J. Opt. Soc. Am. B. 12, No.11, 2101 (1995).

3 J.A. Armstrong, N. Bloembergen, J. Ducuing, and P.S. Pershan, Phys. Rev. 127, NO.6, 1918 (1962); N. Bloembergen and A.J. Sievers, Appl. Phys. Lett. 17, N0.11, 483 (1970).

4 W.R. Bosenberg, A. Drobshoff, L.E. Myers, TOPS Vol.1, Advanced Solid State Lasers, Ed. by S. A. Payne and C.R. Pollock, OSA, 1996, P.32

5 The second reference in Ref. 2.

6 These tuning curves were calculated and created using a program “SNLO Nonlinear Optics” from Arlee V. Smith of Sandia National Labs and Sellmeier equations from Dieter H. Jundt of Crystal Technology, Inc.

7 H. Komine, J.M. Fukumoto, W.H. Long, Jr. and E.A. Stappaerts, "IEEE J. of Selected Topics in Quant. Elect. Vol. 1, NO.1 April 1995, P. 44

8 Handbook of Nonlinear Optical Crystals, V.G. Dmitriev, G.G. Gurzadyan, D.N. Nikogosyan, Springer-Verlag.